Inorg. Chem. **2001,** *40,* 3435−3442

Syntheses, Photophysics, and Photochemistry of Trinuclear Copper(I) Thiolate and Hexanuclear Copper(I) Selenolate Complexes: X-ray Crystal Structures of $[Cu_6(\mu\text{-dppm})_4(\mu_3\text{-SePh})_4](BF_4)_2$ and $[Cu_6\{\mu\text{-}(Ph_2P)_2NH\}_4(\mu_3\text{-SePh})_4](BF_4)_2$

Vivian Wing-Wah Yam,* Chi-Ho Lam, Wendy Kit-Mai Fung, and Kung-Kai Cheung

Department of Chemistry, The University of Hong Kong, Pokfulam Road,
Hong Kong, People's Republic of China

Received November 8, 2000

A series of trinuclear copper(I) thiolate complexes, $[Cu_3(\mu\text{-dppm})_3(\mu_3\text{-SR})_2]BF_4$ (R = C_6H_4Cl-4, $C_6H_4CH_3$-4, $C_6H_4OCH_3$-4, $C_6H_4(OCH_3)_2$-3,4, C_6H_4-benzo-15-crown-5, or ^{t}Bu), $[Cu_3(\mu\text{-dppm})_3(\mu_3\text{-S}^t\text{Bu})](BF_4)_2$, and $[Cu_3(\mu\text{-dppm})_3(\mu_3\text{-SR})(\mu_3\text{-Cl})]BF_4$ (R = $C_6H_4CH_3$-4, $C_6H_4{}^t$Bu-4, or $C_6H_4(CH_3)_3$-2,4,6) and two hexanuclear copper(I) selenolate complexes, $[Cu_6(\mu\text{-P^\wedge P})_4(\mu_3\text{-SePh})_4](BF_4)_2$ (P^P = dppm, $(Ph_2P)_2NH$), have been synthesized, and their photophysical properties have been studied. The X-ray crystal structures of both copper(I) selenolate complexes have been determined. These complexes have been shown to exhibit long-lived low-energy emission in solution, attributed to an excited state of predominantly ligand-to-metal charge-transfer [chalcogenolate to copper(I)] origin.

Introduction

Transition metal thiolate complexes have been well-studied because of their wide applications.[1] Sulfur-containing transition metal complexes are well-known as good catalysts for hydrosulfuriation, hydronitrification, hydrogenation, isomerization, and dehydration of fossil fuels.[2] In addition, sulfur-containing metalloproteins such as the copper B site of cytochrome oxidase, blue copper proteins, and iron−sulfur proteins play an important role in biological systems and are crucial to the development of transition metal thiolate chemistry.[3] Extension of the studies on metal thiolate chemistry to its higher congeners of selenolate and tellurolate has also been widely reported.[4] The potential applications of the transition metal chalcogenolate complexes in electronics such as superconductive and photovoltaic materials have also received increasing attention.[5] As part of our efforts in searching for new luminescent polynuclear metal complexes,[6] we have extended our work on polynuclear copper(I) acetylide complexes with rich luminescence properties[6a,b,d,7] toward copper(I) chalcogenolates. The chalcogenolate in many aspects appears to resemble the acetylide, in that they both are good σ-donors and are capable of displaying a great diversity of structure and bonding modes. Herein, we report the syntheses and luminescence behavior of a series of trinuclear copper(I) thiolate complexes, $[Cu_3(\mu\text{-dppm})_3(\mu_3\text{-SR})_2]BF_4$ (R = C_6H_4Cl-4 (**2**), $C_6H_4CH_3$-4 (**3**), $C_6H_4OCH_3$-4 (**4**), $C_6H_4(OCH_3)_2$-3,4 (**5**), C_6H_4-benzo-15-crown-5 (**6**), and ^{t}Bu (**7**)), $[Cu_3(\mu\text{-dppm})_3(\mu_3\text{-S}^t\text{Bu})](BF_4)_2$ (**8**), $[Cu_3(\mu\text{-dppm})_3(\mu_3\text{-SR})(\mu_3\text{-Cl})]BF_4$ (R = $C_6H_4CH_3$-4 (**9**), $C_6H_4{}^t$Bu-4 (**10**), $C_6H_4(CH_3)_3$-2,4,6 (**11**)), and two hexanuclear copper(I) selenolate complexes, $[Cu_6(\mu\text{-P^\wedge P})_4(\mu_3\text{-SePh})_4](BF_4)_2$ (P^P = dppm (**12**) and $(Ph_2P)_2NH$ (**13**)). The X-ray crystal structures of both copper(I) selenolate complexes **12** and **13** have been determined.

---

(1) (a) Sellmann, D.; Geipel, F.; Moll, M. *Angew. Chem., Int. Ed.* **2000**, *39*, 561. (b) Stephan, D. W.; Nadasdi, T. T. *Coord. Chem. Rev.* **1996**, *147*, 147. (c) Dance, I. G. *Polyhedron* **1986**, *5*, 1037. (d) Blower, P. J.; Dilworth, J. R. *Coord. Chem. Rev.* **1987**, *76*, 121.

(2) (a) *Catalysis*; Mitchell, P. C. H., Kemball, C., Eds.; The Chemical Society: London, 1977; Vol. 1, p 223; Vol. 4, p 203. (b) Topsoe, H.; Clause, B. S. *Catal. Rev.-Sci. Eng.* **1984**, *26*, 395.

(3) (a) Liaw, W. F.; Lee, N. H.; Chen, C. H.; Lee, C. M.; Lee, G. H.; Peng, S. M. *J. Am. Chem. Soc.* **2000**, *122*, 488. (b) Liu, C. W.; Staples, R. J.; Fackler, J. P. *Coord. Chem. Rev.* **1998**, *174*, 147. (c) Ellison, J. J.; Nienstedt, A.; Shoner, S. C.; Barnhart, D.; Cowen, J. A.; Kovacs, J. A. *J. Am. Chem. Soc.* **1998**, *120*, 5691. (d) Ferguson-Miller, S.; Babcock, G. T. *Chem. Rev.* **1996**, *96*, 2889. (e) Ramirez, B. E.; Malmström, B. G.; Winkler, J. R.; Gray, H. B. *Proc. Natl. Acad. Sci. U.S.A.* **1995**, *92*, 11949. (f) Dance, I. G.; Fisher, K. *Prog. Inorg. Chem.* **1994**, *41*, 637. (g) Ueyama, N.; Oku H.; Nakamura, A. *J. Am. Chem. Soc.* **1992**, *114*, 7310. (h) Malmström, B. G. *Chem. Rev.* **1990**, *90*, 1247. (i) Gowik P. K.; Klaoietke, T. M. *Inorg. Chim. Acta* **1990**, *169*, 1. (j) Hollander, I. J.; Shen, Y. Q.; Heim, J.; Demin A. L.; Wolf, S. *Science* **1984**, *224*, 610.

(4) (a) Narayan, S.; Jain, V. K.; Panneerselvam, K.; Lu, T. H.; Tung, S. F. *Polyhedron* **1999**, *18*, 1253. (b) Mashima, K.; Kaneko S.; Tani, K.; Kaneyoshi, H.; Nakamura, A. *J. Organomet. Chem.* **1997**, *546*, 345. (c) Bonasia, P. J.; Christou, V.; Arnold, J. *J. Am. Chem. Soc.* **1993**, *115*, 6777.

(5) (a) Park, Y.; Degroot, D. C.; Schindler, J.; Kannewurf, C. R.; Kanatzidis, M. G. *Chem. Mater.* **1993**, *5*, 8. (b) Moreland, A. C.; Rauchfuss, T. B. *J. Am. Chem. Soc.* **1998**, *120*, 9376. (c) Schmidt, M.; Contakes, S. M.; Rauchfuss, T. B. *J. Am. Chem. Soc.* **1999**, *121*, 9736.

(6) (a) Yam, V. W. W. *J. Photochem. Photobiol. A* **1997**, *106*, 75. (b) Yam, V. W. W.; Lo, K. K. W.; Fung, W. K. M.; Wang, C. R. *Coord. Chem. Rev.* **1998**, *171*, 17. (c) Yam, V. W. W.; Lo, K. K. W. *Comments Inorg. Chem.* **1997**, *19*, 209. (d) Yam, V. W. W.; Lo, K. K. W. *Chem. Soc. Rev.* **1999**, *28*, 323 and reference therein.

(7) (a) Yam, V. W. W.; Lee, W. K.; Lai, T. F. *Organometallics* **1993**, *12*, 2383. (b) Yam, V. W. W.; Lee, W. K.; Yeung, P. K. Y.; Phillips, D. *J. Phys. Chem.* **1994**, *98*, 7545. (c) Yam, V. W. W.; Lee, W. K.; Cheung, K. K.; Crystall, B.; Phillips, D. *J. Chem. Soc., Dalton Trans.* **1996**, 3283. (d) Yam, V. W. W.; Lee, W. K.; Cheung, K. K. *J. Chem. Soc., Dalton Trans.* **1996**, 2335. (e) Yam, V. W. W.; Choi, S. W. K.; Chan, C. L.; Cheung, K. K. *Chem. Commun.* **1996**, 2067. (f) Yam, V. W. W.; Fung, W. K. M.; Wong, M. T. *Organometallics* **1997**, *16*, 1772. (g) Yam, V. W. W.; Fung, W. K. M.; Cheung, K. K. *Chem. Commun.* **1997**, 963. (h) Yam, V. W. W.; Fung, W. K. M.; Wong, M. T. *Organometallics* **1997**, *16*, 1772. (i) Yam, V. W. W.; Fung, W. K. M.; Cheung, K. K. *Organometallics* **1998**, *17*, 3293. (j) Yam, V. W. W.; Lo, K. K. W.; Fung, W. K. M.; Wang, C. R. *Chem. Phys. Lett.* **1998**, *296*, 505. (k) Yam, V. W. W.; Fung, W. K. M.; Cheung, K. K. *J. Cluster Sci.* **1999**, *10*, 37. (l) Yam, V. W. W.; Lo, K. K. W.; Wong, K. M. C. *J. Organomet. Chem.* **1999**, *578*, 3.

10.1021/ic0012322 CCC: $20.00

Experimental Section

Materials. 4-Chlorothiophenol, 4-*tert*-butylthiophenol, and *p*-thiocresol were obtained from Lancaster Synthesis Ltd. 2,4,6-Trimethylthiophenol was purchased from Maybridge Chemical Co. Ltd. 3,4-Dimethoxybenzenethiol was obtained from Lancaster Synthesis Ltd. Phenylselenol and *N*,*N*-bis(diphenylphosphino)amine were obtained from Strem Chemicals Inc. 4-Methoxybenzenethiol was obtained from Maybridge Chemical Co. Ltd. Sodium *tert*-butylthiolate was obtained from Sigma-Aldrich Co. 4-Mercaptobenzo-15-crown-5 was synthesized by a reported procedure.[8] $[Cu(MeCN)_4]PF_6$,[9] $[Cu(MeCN)_4]BF_4$,[9] $[Cu_2(\mu\text{-dppm})_2(MeCN)_2](BF_4)_2$,[10a] $[Cu_2(\mu\text{-dppm})_2(MeCN)_2](PF_6)_2$,[10a] and $[Cu_3(\mu\text{-dppm})_3(\mu_3\text{-Cl})_2]PF_6$[10b] were prepared according to the literature procedures. All solvents were purified and distilled before use using standard procedures.[11] All other reagents were of analytical grade and were used as received.

Syntheses. All reactions were carried out under anaerobic and anhydrous conditions using standard Schlenk techniques.

$[Cu_2\{\mu\text{-}(Ph_2P)_2NH\}_2(MeCN)_2](BF_4)_2$ (1). A dichloromethane solution (30 mL) of $[Cu(MeCN)_4]BF_4$ (0.30 g, 1 mmol) and $(Ph_2P)_2NH$ (0.39 g, 1 mmol) was stirred at room temperature for 24 h to give a colorless solution. The solution was then filtered and evaporated to dryness. The residue was extracted with acetone, and subsequent diffusion of diethyl ether vapor into the acetone solution gave colorless crystals of **1** (73% yield, 0.42 g). UV−Vis (CH_2Cl_2) λ, nm (ϵ_{max}, dm^3 mol^{-1} cm^{-1}): 244sh (38 630), 320sh (11 060). ^{1}H NMR (300 MHz, acetone-d_6, 298 K): δ 2.1 (s, 6H, MeCN), 6.7 (m, 2H, -NH-), 7.4−7.6 (m, 40H, -Ph). ^{31}P{^{1}H} NMR (202 MHz, acetone-d_6, 298 K): δ 49.6. Positive FAB−MS (*m*/*z*): [M − 2MeCN − BF$_4$]$^+$ 985. Anal. Calcd for $Cu_2C_{52}H_{48}P_4N_4B_2F_8$: C, 54.14; H, 4.19; N, 4.86. Found: C, 54.23; H, 4.32; N, 4.95.

$[Cu_3(\mu\text{-dppm})_3(\mu_3\text{-SC}_6H_4Cl\text{-}4)_2]BF_4$ (2). To a solution of $[Cu_2(\mu\text{-dppm})_2(MeCN)_2](BF_4)_2$ (0.38 g, 0.3 mmol) in acetone (40 mL) was added a solution of the triethylammonium salt of 4-ClC_6H_4SH (57.8 mg, 0.4 mmol) in THF (10 mL) (prepared in situ by treatment of a solution of 4-ClC_6H_4SH in THF with an excess of triethylamine (25.3 mg, 0.25 mmol)) at room temperature. The mixture was stirred for 12 h at room temperature. After being evaporated to dryness, the solid residue was extracted with CH_2Cl_2. Subsequent diffusion of diethyl ether vapor into the concentrated solution resulted in the formation of colorless crystals of **2** (75% yield, 0.26 g). UV−Vis (CH_2Cl_2) λ, nm (ϵ_{max}, dm^3 mol^{-1} cm^{-1}): 244sh (45 850), 282sh (37 540). ^{1}H NMR (300 MHz, acetone-d_6, 298 K): δ 3.5 (m, 6H, -CH$_2$-), 6.8−7.7 (m, 68H, -Ph). ^{31}P{^{1}H} NMR (202 MHz, acetone-d_6, 298 K): δ −13.4. Positive FAB−MS (*m*/*z*): [M − BF$_4$]$^+$ 1629. Anal. Calcd for $C_{87}H_{74}P_6S_2Cl_2BF_4Cu_3\cdot H_2O$: C, 60.18; H, 4.38. Found: C, 60.23; H, 4.49.

$[Cu_3(\mu\text{-dppm})_3(\mu_3\text{-SC}_6H_4CH_3\text{-}4)_2]BF_4$ (3). This was prepared by the method similar to that for **2** except 4-$CH_3C_6H_4SH$ (49.6 mg, 0.4 mmol) was used in place of 4-ClC_6H_4SH. Yellow crystals of **3** were obtained (80% yield, 0.27 g). The preparation of **3** has been reported previously by a different synthetic route.[12] UV−Vis (CH_2Cl_2) λ, nm (ϵ_{max}, dm^3 mol^{-1} cm^{-1}): 260sh (12 340) 290sh (11 080). ^{31}P{^{1}H} NMR (202 MHz, acetone-d_6, 298 K): δ −13.7.

$[Cu_3(\mu\text{-dppm})_3(\mu_3\text{-SC}_6H_4\text{-OCH}_3\text{-}4)_2]BF_4$ (4). This was prepared by the method similar to that for **2** except $HSC_6H_4OCH_3$-4 (49.6 mg, 0.4 mmol) was used in place of 4-ClC_6H_4SH. Colorless crystals of **4** were obtained (50% yield, 0.17 g). UV−Vis (CH_2Cl_2) λ, nm (ϵ_{max}, dm^3 mol^{-1} cm^{-1}): 252sh (58 520), 276sh (53 700). ^{1}H NMR (300 MHz, acetone-d_6, 298 K): δ 3.5 (m, 6H, -CH$_2$-), 3.9 (s, 6H, -OCH$_3$), 6.8 (d, 4H, J = 8.7 Hz, -C$_6$H$_4$-), 6.9−7.3 (m, 60H, -Ph), 7.4 (d, 4H, J = 8.7 Hz, -C$_6$H$_4$-). ^{31}P{^{1}H} NMR (202 MHz, acetone-d_6, 298 K): δ −13.9. Positive FAB−MS (*m*/*z*): [M − BF$_4$]$^+$ 1621. Anal. Calcd for $Cu_3C_{89}H_{80}O_2P_6S_2BF_4\cdot 1/2CH_2Cl_2$: C, 61.96; H, 4.69. Found: C, 61.86; H, 4.97.

$[Cu_3(\mu\text{-dppm})_3(\mu_3\text{-SC}_6H_3(OCH_3)_2\text{-}3,4)_2]BF_4$ (5). This was prepared by a method similar to that of **2** except $HSC_6H_3(OCH_3)_2$-3,4 (0.067 g, 0.4 mmol) was used in place of 4-ClC_6H_4SH. Colorless crystals of **5** were obtained (23% yield, 0.080 g). UV−Vis (CH_2Cl_2) λ, nm (ϵ_{max}, dm^3 mol^{-1} cm^{-1}): 278sh (48 400). ^{1}H NMR (300 MHz, acetone-d_6, 298 K): δ 3.2 (s, 6H, -OCH$_3$), 3.4 (m, 6H, -CH$_2$-), 3.9 (s, 6H, -OCH$_3$), 6.8−7.4 (m, 66H, -Ph). ^{31}P{^{1}H} NMR (202 MHz, acetone-d_6, 298K): δ −13.9. Positive FAB−MS (*m*/*z*): [M − BF$_4$]$^+$ 1682. Anal. Calcd for $Cu_3C_{91}H_{84}O_4P_6S_2BF_4$: C, 61.72; H, 4.79. Found: C, 61.46; H, 4.88.

$[Cu_3(\mu\text{-dppm})_3(\mu_3\text{-}S\text{-benzo-15-crown-5})_2]BF_4$ (6). This was prepared by a method similar to that of **2** except 4-mercapto-benzo-15-crown-5 (0.117 g, 0.4 mmol) was used in place of 4-ClC_6H_4SH. Colorless crystals of **6** were obtained (67% yield, 0.27 g). UV−Vis (CH_2Cl_2) λ, nm (ϵ_{max}, dm^3 mol^{-1} cm^{-1}): 276sh (53 030), 292sh (46 770). ^{1}H NMR (300 MHz, acetone-d_6, 298 K): δ 3.5 (t, 4H, J = 5 Hz, -OC*H*$_2$CH$_2$-*p*), 3.6 (m, 6H, P-CH$_2$-P), 3.8 (m, 20H, -OCH$_2$C*H*$_2$O-*p* and CH$_2$-OC*H*$_2$C*H*$_2$O-CH$_2$), 4.0 (t, 4H, J = 5 Hz, -OCH$_2$C*H*$_2$-*m*), 4.3 (t, 4H, J = 5 Hz, -OC*H*$_2$CH$_2$-*m*), 6.8−7.2 (m, 66H, -Ph). ^{31}P{^{1}H} NMR (202 MHz, acetone-d_6, 298 K): δ −13.8. Positive FAB−MS (*m*/*z*): [M − BF$_4$]$^+$ 1944. Anal. Calcd for $Cu_3C_{103}H_{104}O_{10}P_6S_2BF_4\cdot 1/2CH_2Cl_2$: C, 59.95; H, 5.07. Found: C, 59.65; H, 4.87.

$[Cu_3(\mu\text{-dppm})_3(\mu_3\text{-S}^t\text{Bu})_2]BF_4$ (7). This was prepared by the reaction of $[Cu_2(\mu\text{-dppm})_2(MeCN)_2](BF_4)_2$ (0.1 g, 0.09 mmol) with NaS^{t}Bu (0.043 g, 0.4 mmol) in CH_2Cl_2/MeOH (45:15 mL). The mixture was stirred at room temperature for 24 h. After being evaporated to dryness, the solid residue was extracted with acetone. Subsequent diffusion of diethyl ether vapor into the concentrated solution resulted in the formation of colorless crystals of **7** (59% yield, 0.19 g). UV−Vis (CH_2Cl_2) λ, nm (ϵ_{max}, dm^3 mol^{-1} cm^{-1}): 252sh (44 340), 294sh (29 600). ^{1}H NMR (300 MHz, acetone-d_6, 298 K): δ 1.4 (s, 18H, ^{t}Bu), 3.7 (m, 6H, -CH$_2$-), 7.0−7.5 (m, 60H, -Ph). ^{31}P{^{1}H} NMR (202 MHz, acetone-d_6, 298 K): δ −16.9. Positive FAB−MS (*m*/*z*): [M − BF$_4$]$^+$ 1522. Anal. Calcd for $Cu_3C_{83}H_{84}P_6S_2BF_4$: C, 61.96; H, 5.26. Found: C, 62.10; H, 5.38.

$[Cu_3(\mu\text{-dppm})_3(\mu_3\text{-S}^t\text{Bu})](BF_4)_2$ (8). This was prepared by the reaction of $[Cu_2(\mu\text{-dppm})_2(MeCN)_2](BF_4)_2$ (0.1 g, 0.09 mmol) with NaS^{t}Bu (0.007 g, 0.06 mmol) in CH_2Cl_2 (25 mL). The mixture was stirred at room temperature for 24 h. After being evaporated to dryness, the solid residue was extracted with acetone. Subsequent addition of *n*-hexane into the concentrated solution resulted in the formation of yellow crystals of **8** (70% yield, 0.067 g). UV−Vis (CH_2Cl_2) λ, nm (ϵ_{max}, dm^3 mol^{-1} cm^{-1}): 262sh (41 110). ^{1}H NMR (300 MHz, acetone-d_6, 298 K): δ 1.4 (s, 9H, ^{t}Bu), 3.8 (m, 3H, P-C*H*H-P), 4.1 (m, 3H, P-CH*H*-P), 7.0−7.4 (m, 60H, -Ph). ^{31}P{^{1}H} NMR (202 MHz, acetone-d_6, 298 K): δ −11.9. Positive FAB−MS (*m*/*z*): [M − BF$_4$]$^+$ 1520. Anal. Calcd for $Cu_3C_{79}H_{75}P_6SB_2F_8$: C, 59.06; H, 4.71. Found: C, 58.76; H, 4.69.

$[Cu_3(\mu\text{-dppm})_3(\mu_3\text{-SC}_6H_4CH_3\text{-}4)(\mu_3\text{-Cl})]PF_6$ (9). To a solution of $[Cu_3(\mu\text{-dppm})_3(\mu_3\text{-Cl})_2]PF_6$ (0.39 g, 0.25 mmol) in THF (40 mL) was added a solution at room temperature of the sodium salt of *p*-$CH_3C_6H_4SH$ (0.12 g, 1 mmol) in THF (10 mL) (prepared in situ by treatment of a solution of *p*-$CH_3C_6H_4SH$ in THF with NaH and filtering the resulting suspension after the suspension was stirred for 30 min). The mixture was stirred for 12 h at room temperature. After being evaporated to dryness, the solid residue was extracted with acetone. Subsequent diffusion of diethyl ether vapor into the concentrated solution resulted in the formation of colorless crystals of **9** (80% yield, 0.33 g). UV−Vis (CH_2Cl_2) λ, nm (ϵ_{max}, dm^3 mol^{-1} cm^{-1}): 252sh (43 070). ^{1}H NMR (300 MHz, CDCl$_3$, 298 K): δ 2.5 (s, 3H, -CH$_3$), 3.2 (m, 6H, -CH$_2$-), 6.8−7.3 (m, 64H, -Ph). ^{31}P{^{1}H} NMR (202 MHz, acetone-d_6, 298 K): δ −13.6. Positive FAB−MS (*m*/*z*): [M − BF$_4$]$^+$ 1503. Anal. Calcd for $Cu_3C_{82}H_{73}P_7SClF_6$: C, 59.78; H, 4.47. Found: C, 59.58; H, 4.54.

$[Cu_3(\mu\text{-dppm})_3(\mu_3\text{-SC}_6H_4{}^t\text{Bu-4})(\mu_3\text{-Cl})]PF_6$ (10). This was prepared by a method similar to that for **9** except *p*-^{t}BuC$_6$H$_4$SH (0.17 g, 1 mmol) was used in place of *p*-$CH_3C_6H_4SH$. Colorless crystals of **10** were obtained (85% yield, 0.36 g). UV−Vis (CH_2Cl_2) λ, nm (ϵ_{max}, dm^3 mol^{-1} cm^{-1}): 252sh (39 580), 290sh (22 800). ^{1}H NMR (300 MHz, CDCl$_3$, 298 K): δ 1.6 (s, 9H, ^{t}Bu), 3.4 (m, 6H, -CH$_2$-), 6.7−7.4 (m, 64H, -Ph). ^{31}P{^{1}H} NMR (202 MHz, acetone-d_6, 298 K): δ −13.6. Positive

---

(8) Shinkai, S.; Minami, T.; Araragi, Y.; Manabe, O. *J. Chem. Soc., Perkin Trans. 2* **1985**, 503.

(9) Kubas, G. J. *Inorg. Synth*. **1979**, *19*, 90.

(10) (a) Diéz, J.; Gamasa, M. M. P.; Gimeno, J.; Tiripicchio, A.; Camellini, M. T. *J. Chem. Soc., Dalton Trans*. **1987**, 1275, 172. (b) Marsich, N.; Camus, A.; Cebulec, E. *J. Inorg. Nucl. Chem*. **1972**, *34*, 933.

(11) Perrin, D. D.; Armarego, W. L. F.; Perrin, D. R. *Purification of Laboratory Chemicals*, 2nd ed.; Pergamon: Oxford, UK, 1980.

(12) Diéz, J.; Gamasa, M. P.; Gimeno, J. *Polyhedron* **1995**, *14*, 741.

FAB−MS (*m*/*z*): [M$^+$] 1545. Anal. Calcd for $Cu_3C_{85}H_{79}P_7SClF_6$: C, 60.43; H, 4.71. Found: C, 60.42; H, 4.78.

$[Cu_3(\mu\text{-dppm})_3(\mu_3\text{-SC}_6H_2(CH_3)_3\text{-2,4,6})(\mu_3\text{-Cl})]PF_6$ (11). This was prepared by a method similar to that for **9**, except 2,4,6-$(CH_3)_3C_6H_2$-SH (0.15 g, 1 mmol) was used instead. Air-stable white crystals of **11** were obtained (90% yield, 0.38 g). UV−Vis (CH_2Cl_2) λ, nm (ϵ_{max}, dm^3 mol^{-1} cm^{-1}): 250sh (46 160), 280sh (30 270). ^{1}H NMR (300 MHz, acetone-d_6, 298 K): δ 2.2 (s, 6H, -CH$_3$ of 2,4,6-trimethylthiophenolate *ortho* to S), 2.3 (m, 3H, -CH$_3$ of 2,4,6-trimethylthiophenolate *para* to S), 3.6 (m, 6H, -CH$_2$-), 6.8−7.8 (m, 62H, -Ph). ^{31}P{^{1}H} NMR (202 MHz, acetone-d_6, 298 K): δ −15.1. Positive FAB−MS (*m*/*z*): [M − BF$_4$]$^+$ 1529. Anal. Calcd for $Cu_3C_{84}H_{77}P_7SClF_6\cdot 2(CH_3)_2CO$: C, 60.63; H, 4.97. Found: C, 60.98; H, 4.97.

$[Cu_6(\mu\text{-dppm})_4(\mu_3\text{-SePh})_4](BF_4)_2$ (12). This was prepared by the method similar to that of **2** except HSePh (0.063 g, 0.4 mmol) was used in place of 4-ClC_6H_4SH. Addition of diethyl ether into the concentrated CH_2Cl_2 solution gave yellow crystals of **12** (30% yield, 0.083 g). UV−Vis (CH_2Cl_2) λ, nm (ϵ_{max}, dm^3 mol^{-1} cm^{-1}): 268sh (82 830). ^{1}H NMR (300 MHz, CD_2Cl_2, 298 K): δ 3.0 (m, 8H, -CH$_2$-), 6.4−7.4 (m, 100H, -Ph). ^{31}P{^{1}H} NMR (202 MHz, CD_2Cl_2, 298 K): δ −12.4, −16.8. Positive FAB−MS (*m*/*z*): [M − BF$_4$]$^+$ 2632. Anal. Calcd for $Cu_6C_{124}H_{108}P_8Se_4B_2F_8\cdot CH_2Cl_2$: C, 54.60; H, 3.97. Found: C, 54.30; H, 4.09.

$[Cu_6\{\mu\text{-}(Ph_2P)_2NH\}_4(\mu_3\text{-SePh})_4](BF_4)_2$ (13). This was prepared by the method similar to that of **12** except $[Cu_2(\mu\text{-}(Ph_2P)_2NH)_2(MeCN)_2](BF_4)_2$ (0.33 g, 0.3 mmol) was used in place of $[Cu_2(\mu\text{-dppm})_2(MeCN)_2](BF_4)_2$. Pale yellow crystals of **13** were obtained (42% yield, 0.113 g). UV−Vis (CH_2Cl_2) λ, nm (ϵ_{max}, dm^3 mol^{-1} cm^{-1}): 270sh (73 890), 294sh (55 490). ^{1}H NMR (300 MHz, CD_2Cl_2, 298 K): δ 3.7 (m, 4H, -NH-), 6.5−7.4 (m, 100H, -Ph). ^{31}P{^{1}H} NMR (202 MHz, acetone-d_6, 298 K): δ 33.1, 38.7. Positive FAB−MS (*m*/*z*): [M − BF$_4$]$^+$ 2636. Anal. Calcd for $Cu_6C_{120}H_{104}P_8N_4Se_4B_2F_8\cdot CH_2Cl_2$: C, 51.80; H, 3.81; N, 2.00. Found: C, 51.70; H, 3.88; N, 1.98.

Physical Measurements. Raman spectra were recorded as solid samples on a Bio-Rad FT-Raman spectrometer with the 1064 nm line of a Nd:YAG laser as the excitation source. ^{1}H and ^{31}P NMR spectra were recorded on Bruker DRX-300 (300 MHz) and Bruker DRX-500 (202 MHz) multinuclear FT-NMR spectrometers, respectively. Chemical shifts (δ, ppm) were reported relative to tetramethylsilane (Me_4Si) for ^{1}H and 85% H_3PO_4 for ^{31}P NMR spectroscopy. UV−Vis spectra were obtained on a Hewlett-Packard 8452A diode array spectrophotometer. Positive ion FAB mass spectra were recorded on a Finnigan MAT95 mass spectrometer. Elemental analyses of the newly synthesized complexes were performed on a Carlo Erba 1106 elemental analyzer at the Institute of Chemistry, Chinese Academy of Sciences. The crystal structures of **12** and **13** were determined on a MAR diffractometer equipped with an image plate detector.

Steady-state emission and excitation spectra at room temperature and at 77 K were obtained on a Spex Fluorolog-2 model F111 fluorescence spectrophotometer equipped with a Hamamatsu R928 PMT detector. The 77 K solid-state emission and excitation spectra were recorded with solid samples loaded in a quartz tube inside a quartz-walled optical Dewar flask filled with liquid nitrogen. Room temperature spectra were recorded similarly but without liquid nitrogen inside the Dewar flask. For solution photophysical measurements, the sample solutions were degassed on a high vacuum line in a two-compartment cell consisting of a 10-mL Pyrex bulb and a 1-cm path length quartz cuvette and sealed from the atmosphere by a Bibby Rotaflo HP6 Teflon stopper. The solutions were subject to at least four freeze−pump−thaw cycles. Emission lifetime measurements were performed using a conventional laser system. The excitation source was the 355-nm output (third harmonic) of a Spectra-Physics Quanta-Ray Q-switched GCR-150-10 pulsed Nd:YAG laser. Luminescence decay signals were detected by a Hamamatsu R928 PMT and recorded on a Tektronix model TDS-620A (500 MHz, 2GS/s) digital oscilloscope and analyzed using a program for exponential fits. Time-resolved transient absorption spectroscopy was performed using the 355-nm output (third harmonic) of the Spectra-Physics Quanta-Ray Q-switched GCR-150-10 pulsed Nd:YAG laser as the excitation source, with the monitoring light beam generated from a 250-W quartz−tungsten−halogen lamp placed perpendicular to the excitation beam. The output of the quartz−tungsten−halogen lamp was wavelength selected by passing through two monochromators (Oriel 77250, 1/8 m and 77200, 1/4 m). The transient absorption signals were detected by a Hamamatsu R928 photomultiplier tube, and the signal was amplified using a Tektronix AM 502 differential amplifier and digitized on a Tektronix model TDS-620A (500 MHz, 2GS/s) digital oscilloscope interfaced to an IBM personal computer for data acquisition and analysis.

Bimolecular quenching rate constants (k_q) were obtained by time-resolved emission measurements using the Stern−Volmer equation, $\tau_o/\tau = 1 + k_q\tau_o[Q]$, where τ_o and τ are the luminescence lifetimes in the absence and presence of quencher with concentration [Q], respectively.

Crystal Structure Studies. Single crystals of **12** and **13** suitable for X-ray diffraction studies were grown by the layering of diethyl ether on a concentrated acetone solution of the complex.

Crystal Data for $[Cu_6(\mu\text{-dppm})_4(\mu_3\text{-SePh})_4](BF_4)_2$ (12). $[(C_{124}H_{108}P_8Se_4Cu_6)^{2+}\cdot 2BF_4^-]$: formula weight = 2716.73, tetragonal, space group $I\bar{4}$ (No. 82), a = 16.071(3) Å, c = 24.844(3) Å, V = 6416(1) Å^3, Z = 2, D_c = 1.406 g cm^{-3}, μ(Mo Kα) = 22.67 cm^{-1}, F(000) = 2728, T = 301 K. A yellow crystal of dimensions 0.20 × 0.15 × 0.07 mm in a glass capillary was used for data collection at 28 °C on a MAR diffractometer with a 300-mm image plate detector using graphite monochromatized Mo Kα radiation (λ = 0.71073 Å). Data collections were made with 3° oscillations (60 images) at 120-mm distances and 360-s exposures. The images were interpreted, and intensities were integrated using the program *DENZO*.[13a] A total of 2967 unique reflections was obtained from a total of 26 857 measured reflections (R_{int} = 0.063). A total of 2414 reflections with $I > 3\sigma(I)$ was considered observed and used in the structural analysis. These reflections were in the range h, 0−19; k, −13 to 13; and l, 0−28 with $2\theta_{max}$ = 50.8°.

Crystal Data for $[Cu_6\{\mu\text{-}(Ph_2P)_2NH\}_4(\mu_3\text{-SePh})_4](BF_4)_2$ (13). $[(C_{120}H_{104}N_4P_8Se_4Cu_6)^{2+}\cdot 2BF_4^-\cdot 3(CH_3)_2CO]$: formula weight = 2894.92, monoclinic, space group $P2_1$ (No. 4), a = 17.718(3) Å, b = 15.638(3) Å, c = 25.509(3) Å, β = 99.20(2)°, V = 6976(1) Å^3, Z = 2, D_c = 1.378 g cm^{-3}, μ(Mo Kα) = 20.92 cm^{-1}, F(000) = 2920, T = 301 K. A yellow crystal of dimensions 0.25 × 0.20 × 0.07 mm inside a glass capillary was used for data collection at 28 °C on a MAR diffractometer with a 300-mm image plate detector using graphite monochromatized Mo Kα radiation (λ = 0.71073 Å). Data collections were made with 2° oscillations (90 images) at 125-mm distances and 600-s exposures. The images were interpreted, and intensities were integrated using the program *DENZO*.[13a] A total of 11 559 unique reflections was obtained from a total of 53 159 measured reflections (R_{int} = 0.070). A total of 7759 reflections with $I > 3\sigma(I)$ was considered observed and used in the structural analysis. These reflections were in the range h, 0−20; k, 0−18; and l, −30 to 29 with $2\theta_{max}$ = 49.8°.

Structure Determination and Refinement. The space group of **12** was determined based on systematic absences and on a statistical analysis of intensity distribution, and the successful refinement of the structure was solved by direct methods (SIR92)[13b] and expanded by Fourier method and refinement by full-matrix least-squares using the software package TeXsan[13c] on a Silicon Graphics Indy computer. One crystallographic asymmetric unit consists of one-quarter of one formula unit with Cu(1) and both the B atoms at special positions having occupation numbers of 0.5, 0.25, and 0.25, respectively. In the least-squares refinement, all 37 nonhydrogen atoms of the complex cation were refined anisotropically, 4 atoms of the anions were refined isotropically, and 27 H atoms at calculated positions with thermal parameters equal to 1.3× that of the attached C atoms were not refined. Convergence for 331 variable parameters by least-squares refinement on F with $w = 4F_o^2/\sigma^2(F_o^2)$, where $\sigma^2(F_o^2) = [\sigma^2(I) + (0.024F_o^2)^2]$ for

---

(13) (a) DENZO: Gewirth, D. *The HKL Manual*: *A Description of Programs DENZO, XD1SPLAYF, and SCALEPACK*; Yale University: New Haven, 1995. (b) SIR92: Altomare, A.; Cascarano, M.; Giacovazzo, C.; Guagliardi, A.; Burla, M. C.; Polidori, G.; Camalli, M. *J. Appl. Crystallogr.* **1994**, *27*, 435. (c) *TeXsan*: *Crystal Structure Analysis Package*; Molecular Structure Corporation: The Woodlands, TX, 1985, 1992. (d) PATTY: Beurskens, P. T.; Admiral, G.; Beursken, G.; Bosman, W. P.; Garcia-Granda, S.; Gould, R. O.; Smits, J. M. M.; Smykalla, C. *The DIRDIF Program System*; Technical Report of the Crystallography Laboratory; University of Nijmegen: The Netherlands, 1992.

Scheme 1

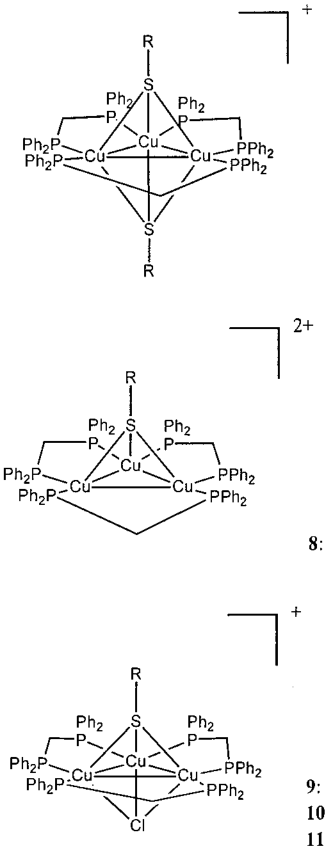

2: R = C_6H_4-Cl-4
3: R = C_6H_4-CH_3-4
4: R = C_6H_4-OCH_3-4
5: R = C_6H_3-$(OCH_3)_2$-3,4
6: R = benzo-15-crown-5
7: R = ^{t}Bu

8: R = ^{t}Bu

9: R = C_6H_4-CH_3-4
10: R = C_6H_4-^{t}Bu-4
11: R = C_6H_2-$(CH_3)_3$-2,4,6

2414 reflections with $I > 3\sigma(I)$ was reached at $R = 0.055$ and $wR = 0.074$ with a goodness-of-fit of 2.50. $(\Delta/\sigma)_{\max} = 0.05$ except for atoms of the anions. The final difference Fourier map was featureless, with maximum positive and negative peaks of 0.67 and 0.43 e$Å^{-3}$, respectively.

The space group of **13** was determined based on systematic absences and on a statistical analysis of intensity distribution, and the successful refinement of structure was solved by Patterson methods and expanded by Fourier methods (PATTY)[13d] and by full-matrix least-squares using the software package TeXsan[13c] on a Silicon Graphics Indy computer. A crystallographic asymmetric unit consists of one formula. In the least-squares refinement, the Cu, Se, P, and N atoms (total 22) were refined anisotropically; the C, O, F, and B atoms (total 142) were refined isotropically; and 118 H atoms at calculated positions with thermal parameters equal to 1.3× that of the attached C atoms were not refined. The 4 H atoms bonded to the 4 N atoms were not included in the calculation. Convergence for 766 variable parameters by least-squares refinement on F with $w = 4F_o^2/\sigma^2(F_o^2)$, where $\sigma^2(F_o^2) = [\sigma^2(I) + (0.033F_o^2)^2]$ for 7759 reflections with $I > 3\sigma(I)$ was reached at $R = 0.079$ and $wR = 0.107$ with a goodness-of-fit of 2.36. $(\Delta/\sigma)_{\max} = 0.05$ except for atoms of the anions and solvent molecules. The final difference Fourier map was featureless, with maximum positive and negative peaks of 1.08 and 0.79 e$Å^{-3}$, respectively.

Results and Discussion

The trinuclear copper(I) thiolate complexes (Scheme 1) were prepared by treatment of $[Cu_2(\mu\text{-dppm})_2(MeCN)_2](BF_4)_2$ with the respective triethylammonium or sodium thiolate in the molar ratio of 3:4 to give **2**−**7** and in the molar ratio of 3:2 to give **8**. Reaction of $[Cu_3(\mu\text{-dppm})_3(\mu_3\text{-Cl})_2]PF_6$ with an excess of the respective sodium thiolate gave **9**−**11**. On the other hand, treatment of $[Cu_2(\mu\text{-P}^\wedge\text{P})_2(MeCN)_2](BF_4)_2$ ($\text{P}^\wedge\text{P}$ = dppm, $(Ph_2P)_2NH$) with triethylammonium phenylselenolate in the molar ratio of 3:4 gave instead the hexanuclear copper(I) complexes **12** and **13**, despite the reaction conditions used were the same as that for the syntheses of the aryl thiolate analogues. The chalcogenolate ligands in all the trinuclear and hexanuclear copper(I) complexes show a μ_3-bridging mode. The propensity of the selenolate in forming hexanuclear complexes rather than trinuclear complexes as in the thiolate analogues may be ascribed to the difference in size of the selenium atom and the sulfur atom. An independent report on the preparation of **3** employing a different route has been published by Gimeno and co-workers.[12] All the newly synthesized complexes gave satisfactory elemental analyses and were characterized by positive FAB−MS, ^{1}H, and ^{31}P NMR spectroscopy.

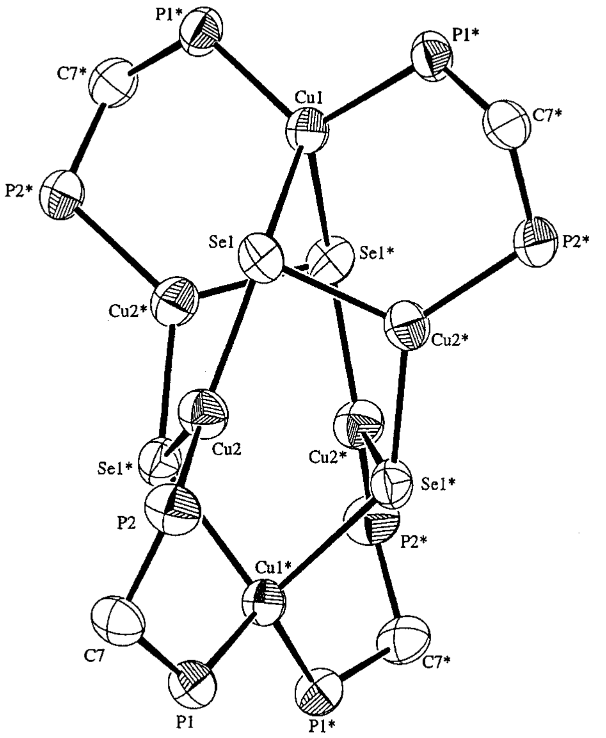

Figure 1. Perspective drawing of the complex cation of **12** with the atomic numbering scheme. Hydrogen atoms and phenyl rings have been omitted for clarity. Thermal ellipsoids are shown at the 30% probability level.

The perspective drawings of the complex cations of **12** and **13** with atomic numbering are depicted in Figures 1 and 2, respectively. The crystal structure determination data for **12** and **13** are given in Table 1. Selected bond distances and angles for **12** and **13** are given in Table 2. The six copper atoms of **12** and **13** are arranged as a structure of two Cu_3 isosceles triangles, with the two Cu_3 planes roughly perpendicular to each other with plane angles 90° and 86.4(2)° in **12** and **13**, respectively. For each Cu_3 triangle, two of the edges were bridged by the dppm ligands. The four selenium atoms showed asymmetric μ_3-bridging mode, with the three Cu−Se bond distances and Cu−Se−Cu bond angles significantly different from each other about each selenium atom. The Cu−Se bond distances are in the range of 2.369(1)−2.565(2) Å and 2.378(3)−2.579(4) Å for **12** and **13**, respectively. The Cu⋯Cu distances are in the range of 3.284(1)−3.325(5) Å and 3.006(4)−3.285(2) Å in the respective complexes **12** and **13**.

The electronic absorption spectra for complexes **2**−**13** in dichloromethane are characterized by absorption shoulders at ca. 250 and 260−295 nm, and the electronic absorption data are summarized in Table 3. The high energy absorption at ca. 250−270 nm is assigned as an intraligand (IL) transition of

Table 1. Crystallographic Data for Hexanuclear Copper(I) Selenolate Complexes

	12	**13**
formula	$\{[Cu_6C_{120}H_{104}N_4P_8Se_4]^{2+}$ $2BF_4^-\}$	$\{[Cu_6C_{120}H_{104}N_4P_8Se_4]^{2+}$ $2BF_4^-\cdot 3(CH_3)_2CO\}$
fw	2716.73	2894.92
T, K	301	301
a, Å	16.071(3)	17.718(3)
b, Å	16.071(3)	15.638(3)
c, Å	24.844(3)	25.509(3)
β, deg	90	99.20(2)
V, Å^3	6416(1)	6976(1)
cryst syst	tetragonal	monoclinic
space group	$I\bar{4}$	$P2_1$
Z	2	2
D_c, g cm^{-3}	1.406	1.378
λ, Å^b	0.71073	0.71073
μ, cm^{-1}	22.67	20.92
R^a	0.055	0.079
wR^a	0.074	0.107

[a] $w = 4F_o^2/[\sigma^2(I) + (aF_o^2)^2]$ with $I > 3\sigma(I)$ (**12**, $a = 0.024$; **13**, $a = 0.033$). [b] Graphite monochromated Mo Kα.

dppm since free dppm absorbs strongly in this region. The absorption shoulders at ca. 290 nm with tails extending to ca. 400 nm are likely to arise from chalcogenolate ligand-centered and chalcogenolate-to-copper ligand-to-metal charge-transfer (LMCT) transitions. Since the electronic absorption spectra were rather featureless, no further attempts were made to unambiguously assign the absorption bands.

Excitation of solid samples and fluid solutions of the polynuclear copper(I) chalcogenolate complexes produced intense long-lived dual luminescence. Their photophysical data are collected in Table 3. Representative emission spectra are shown in Figures 3 and 4.

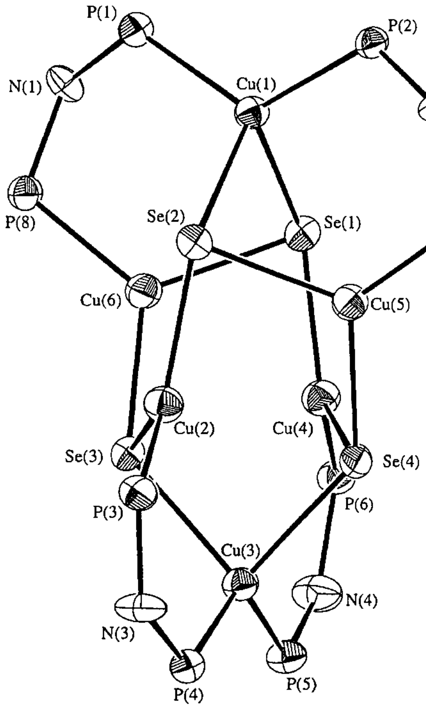

Figure 2. Perspective drawing of the complex cation of **13** with the atomic numbering scheme. Hydrogen atoms and phenyl rings have been omitted for clarity. Thermal ellipsoids are shown at the 45% probability level.

The solid-state emission spectra of complexes **2**−**13** are dominated by a high-energy ligand-centered emission at ca. 430−550 nm, while the emission spectra of degassed acetone solutions of the trinuclear copper(I) thiolate complexes **2**−**11** show a longer-lived low energy emission at ca. 580−640 nm, with emission lifetimes in the microsecond range, suggesting that the emissions are phosphorescence in nature. An emission energy trend of SC_6H_4-Cl-*p* > SC_6H_4-CH_3-*p* ≅ SC_6H_4-OCH_3-*p* ≅ SC_6H_3-$(OCH_3)_2$-3,4 ≅ S-benzo-15-crown-5 > S-^{t}Bu is observed for the bicapped thiolate complexes **2**−**7**. For the mix-capped thiolate complexes **9**−**11**, a solution emission energy trend in the order **9** ≥ **10** > **11** has been observed. This appears to be dependent on the electron-donating ability of the thiolate ligands, and an excited-state origin of largely LMCT [$RS^-\rightarrow Cu_3$] character is favored. Similar assignments have been suggested in a series of d^{10} thiocarbamate complexes, [M_6L_6] (M = Cu, L = mtc; M = Ag, L = mtc, dtc; mtc = di-*n*-propylmonothiocarbamate; dtc = di-*n*-propylthiocarbamate),[14] and a series of copper(I) arenethiolate complexes, [$CuSC_6H_4\{(R)$-$CH(Me)NMe_2\}$-2$]_3$, [$CuSC_6H_4(CH_2NMe_2)$-2$]_3$, [$Cu_3\{SC_6H_4$-

Table 2. Selected Bond Distances (Å) and Angles (deg) with Estimated Standard Deviations in Parentheses for Hexanuclear Copper(I) Selenolate Complexes

Bond Lengths (Å)

12		**13**			
Cu(1)···Cu(2*)	3.325(5)	Cu(1)···Cu(5)	3.285(2)	Cu(2)···Cu(6)	3.155(2)
Cu(2)···Cu(2*)	3.284(1)	Cu(1)···Cu(6)	3.284(1)	Se(3)−Cu(2)	2.417(3)
Cu(1)−Se(1)	2.565(2)	Cu(3)···Cu(2)	3.255(8)	Se(3)−Cu(3)	2.579(4)
Cu(2)−Se(1)	2.414(2)	Cu(3)···Cu(4)	3.244(9)	Se(3)−Cu(6)	2.381(3)
Cu(2)−Se(2*)	2.369(1)	Cu(4)···Cu(5)	3.203(5)	Se(4)−Cu(3)	2.543(4)
Cu(1)−P(1*)	2.297(3)	Cu(4)···Cu(6)	3.006(4)	Se(4)−Cu(4)	2.407(4)
Cu(1*)−P(1)	2.297(3)	Cu(2)···Cu(5)	3.057(1)	Se(4)−Cu(5)	2.378(3)
Cu(2)−P(2)	2.231(3)				

Bond Angles (deg)

12		**13**	
Cu(2)−Cu(1*)−Cu(2*)	72.1(6)	Cu(5)−Cu(1)−Cu(6)	72.1(6)
Cu(1)−Se(1)−Cu(2)	138.43(6)	Cu(4)−Cu(3)−Cu(2)	71.4(9)
Cu(1)−Se(1)−Cu(2*)	83.75(5)	Cu(1)−Se(1)−Cu(4)	136.9(1)
Cu(2)−Se(1)−Cu(2*)	86.85(6)	Cu(1)−Se(1)−Cu(6)	72.1(6)
Se(1)−Cu(1)−P(1*)	120.58(8)	Cu(4)−Se(1)−Cu(6)	77.0(3)
Se(1*)−Cu(1)−P(1*)	105.05(8)	Cu(3)−Se(3)−Cu(6)	135.2(1)
Se(1)−Cu(2*)−P(2*)	128.8(1)	Cu(3)−Se(3)−Cu(2)	80.9(3)
Se(1)−Cu(2)−P(2)	119.6(1)	Cu(6)−Se(3)−Cu(2)	82.2(4)

Table 3. Photophysical Data for Polynuclear Copper(I) Chalcogenolate Complexes

complex	medium (T, K)	emission λ_{em}, nm (τ_o, μs)[a]	electronic abs[c] λ, nm (ϵ_{max}, dm^3 mol^{-1} cm^{-1})
2	acetone (298)	435, 587 (0.18)	244sh (45 850), 282sh (37 540)
	solid (298)	425, 550sh	
	solid (77)	470sh, 550sh	
3	acetone (298)	475sh, 600 (1.42)	260sh(12 340), 290sh (11 080)
	solid (298)	440, 466sh, 550sh	
	solid (77)	476 606[b]	
4	acetone (298)	613 (1.3)[b]	252sh (58 520), 276sh (53 700)
	solid (298)	437, 466sh (0.11)	
	solid (77)	471, 653	
5	acetone (298)	598 (1.3)[b]	278sh (48 400)
	solid (298)	440, 464sh (<0.1)	
	solid (77)	482	
6	acetone (298)	600 (1.1)[b]	276sh (53 030), 292sh (46 770)
	solid (298)	439, 467sh (<0.1)	
	solid (77)	463, 597sh	
7	acetone (298)	637 (5.6)[b]	252sh (44 340), 294sh (29 600)
	solid (298)	436 (<0.1)	
	solid (77)	415	
8	acetone (298)	623 (8.2)[b]	262sh (41 110)
	solid (298)	580 (<0.1)	
	solid (77)	540, 608	
9	acetone (298)	577 (<0.1)	252sh (43 070)
	solid (298)	435, 465sh, 550sh	
	solid (77)	463, 630	
10	acetone (298)	460sh, 603 (0.24)	252sh (39 580), 290sh (22 800)
	solid (298)	440, 550sh	
	solid (77)	462, 600sh	
11	acetone (298)	507, 644 (0.82)	250sh (46 160), 280sh (30 270)
	solid (298)	550sh	
	solid (77)	466, 671	
12	acetone (298)	626 (4.5)[b]	268sh (82 830)
	solid (298)	435, 464sh (<0.1)	
	solid (77)	533	
13	acetone (298)	669sh,[b] 700 (0.9)[b]	270sh (73 890), 294sh (55 490)
	solid (298)	435, 463sh (<0.1)	
	solid (77)	630	

[a] Excitation wavelength at 350 nm. [b] Excitation wavelength at 450 nm. [c] In CH_2Cl_2 solution.

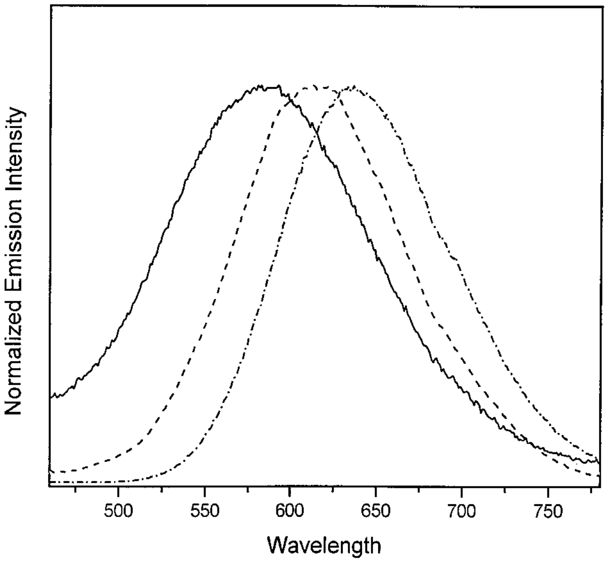

Figure 3. Normalized emission spectra of $[Cu_3(\mu\text{-dppm})_3(\mu_3\text{-SR})_2]BF_4$ (R = C_6H_4Cl-4, **2** (—); $C_6H_4OCH_3$-4, **4** (---); and ^{t}Bu, **7** (—•—)) in degassed acetone at room temperature. Excitation wavelength at 450 nm.

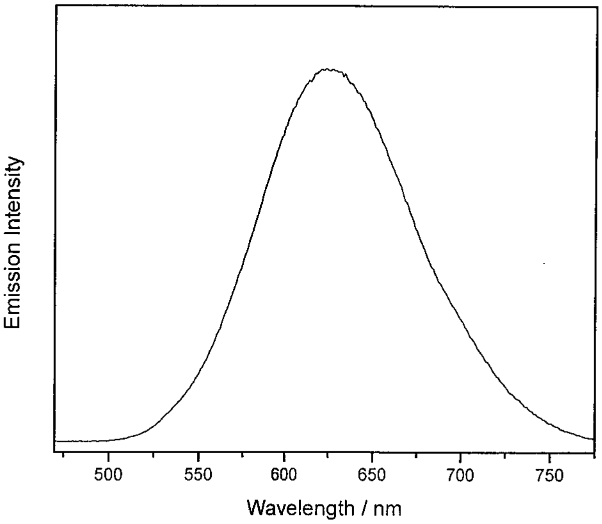

Figure 4. Emission spectrum of **12** in degassed acetone at room temperature. Excitation wavelength at 450 nm.

$[CH(Me)NMe_2]$-2$\}_2(C{\equiv}C\text{-}^tBu)]_2$, and $[Cu_3\{SC_6H_4(CH_2NMe_2)-2\}_2(C{\equiv}C^tBu)]_2$.[15]

Excitation of degassed acetone solutions of **12** and **13** at $\lambda >$ 350 nm produced a low energy emission band at 626 and 700 nm, respectively. The relatively long excited-state lifetime observed suggests that the emission is most likely associated with a spin-forbidden transition of triplet parentage. Given the strong electron-donating ability of the selenolate ligand, it is also likely that the origin of the emission is from states derived from a $[PhSe^- \rightarrow Cu_6]$ LMCT transition. A possible involvement of a copper-centered d−s state has not been ruled out. A similar assignment has also been suggested for other related copper(I) chalcogenide systems, $[M_4(\mu\text{-dppm})_4(\mu_4\text{-E})]^{2+}$ (M = Cu, E = S, Se; M = Ag, E = S, Se, Te), in which a $[E^{2-} \rightarrow Cu_4]$ LMCT origin, mixed with metal-centered d−s/d−p excited states, was assigned.[6,16] Although a chalcogenolate-to-phosphine ligand-to-ligand charge transfer (LLCT) origin may also be possible

---

(14) Sabin, F.; Ryu, C. K.; Ford, P. C.; Vogler, A. *Inorg. Chem.* **1992**, *31*, 1941.

(15) (a) Knotter, D. M.; van Koten, G.; van Maanen, H. L.; Grove, D. M.; Spek, A. L. *Angew. Chem., Int. Ed. Engl.* **1989**, *28*, 341. (b) Knotter, D. M.; van Maanen, H. L.; Grove, D. M.; Spek, A. L.; van Koten, G. *Inorg. Chem.* **1991**, *30*, 3309. (c) Knotter, D. M.; Spek, A. L.; van Koten, G. *J. Chem. Soc., Chem. Commun.* **1989**, 1738. (d) Knotter, D. M.; Spek, A. L.; Grove, D. M.; van Koten, G. *Organometallics* **1992**, *11*, 4083.

(16) (a) Yam, V. W. W.; Lee, W. K. *J. Chem. Soc., Chem. Commun.* **1993**, 1571. (b) Yam, V. W. W.; Lo, K. K. W.; Cheung, K. K. *Inorg. Chem.* **1996**, *35*, 3459. (c) Yam, V. W. W.; Lo, K. K. W.; Wang, C. R. *Inorg. Chem.* **1996**, *35*, 5116. (d) Wang, C. R.; Lo, K. K. W.; Yam, V. W. W. *Chem. Phys. Lett.* **1996**, *262*, 91. (e) Yam, V. W. W.; Lo, K. K. W.; Wang, C. R.; Cheung, K. K. *J. Phys. Chem. A* **1997**, *101*, 4666. (f) Wang, C. R.; Lo, K. K. W.; Yam, V. W. W. *J. Chem. Soc., Dalton Trans.* **1997**, 227. (g) Yam, V. W. W.; Lo, K. K. W.; Fung, W. K. M.; Wang, C. R. *Chem. Phys. Lett.* **1998**, *296*, 505.

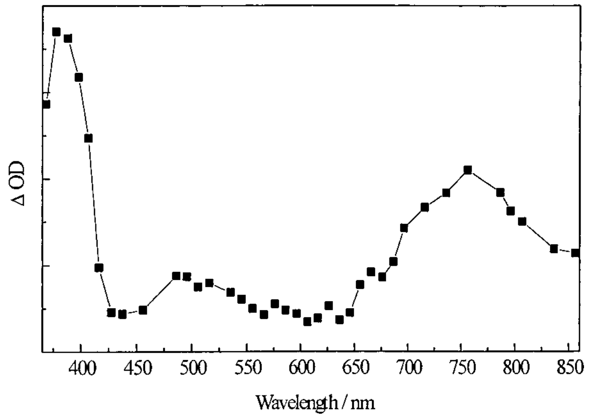

Figure 5. Transient absorption difference spectrum recorded 2 μs after the laser flash for a degassed acetone solution (0.1 M ^{n}Bu$_4$NPF$_6$) of **3** (1.3 × 10^{-4} M) and 4-(methoxycarbonyl)-*N*-methylpyridinium hexafluorophosphate (1.4 × 10^{-2} M).

and would also give rise to a similar energy trend as an origin of predominantly LMCT character, an assignment of such an origin is not favored in view of the close resemblance of the emission energies of **12** and **13**. In conclusion, the origin of the low energy emission is tentatively assigned as derived from an origin of predominantly LMCT [RS$^-$→Cu$_3$] or [PhSe$^-$→Cu$_6$] triplet character.

The trinuclear copper(I) thiolate complexes have been found to be strong reducing agents in the excited state. The phosphorescent state of **3** has been found to be quenched by 4-(methoxycarbonyl)-*N*-methylpyridinium hexafluorophosphate with a bimolecular quenching rate constant k_q of 3.97 × 10^{10} dm^3 mol^{-1} s^{-1}. Laser flash photolysis of a degassed acetone solution (0.1 M ^{n}Bu$_4$NPF$_6$) of **3** with 4-(methoxycarbonyl)-*N*-methylpyridinium salt generated a transient absorption difference spectrum with bands at ca. 390, 500, and 760 nm (Figure 5). The 390 nm band is characteristic of the pyridinyl radical.[17]

From the transient absorption spectroscopy, the reaction of [Cu$_3$(*μ*-dppm)$_3$(*μ*$_3$-SC$_6$H$_4$CH$_3$-*p*)$_2$]BF$_4$ (1.3 × 10^{-4} M) and 4-(methoxycarbonyl)-*N*-methylpyridinium ion (0.014 M) has proved to be electron-transfer in nature, and a proposed mechanism is shown below.

$$[\mathrm{Cu_3(\mu\text{-}dppm)_3(\mu_3\text{-}SC_6H_4CH_3\text{-}}p)_2]^+ + h\nu \rightarrow [\mathrm{Cu_3(\mu\text{-}dppm)_3(\mu_3\text{-}SC_6H_4CH_3\text{-}}p)_2]^{+*}$$

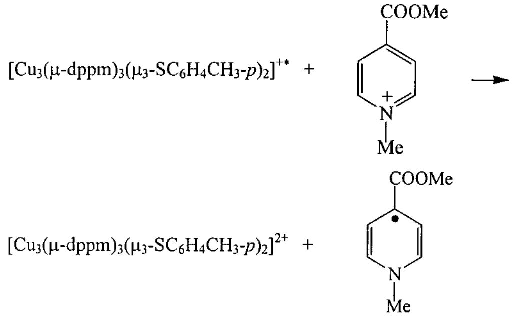

Table 4. Summary of the Electrode Potential for the First Oxidation Couple for Trinuclear and Hexanuclear Copper(I) Chalcogenolate Complexes

complex	oxidation $E_{1/2}$ (V vs SCE)^{a,b}	complex	oxidation $E_{1/2}$ (V vs SCE)^{a,b}
2	+0.72	**8**	+0.54
3	+0.65	**9**	+0.67
4	+0.60	**10**	+0.66
5	+0.59	**11**	+0.62
6	+0.60	**12**	+0.70
7	+0.55	**13**	+0.74

[a] In MeCN (0.1 M ^{n}Bu$_4$NPF$_6$), glassy carbon electrode, scan rate = 100 mV s^{-1}, 298 K. [b] $E_{1/2}$ is taken to be the average of E_{pa} and E_{pc}, where E_{pa} and E_{pc} are the anodic and cathodic peak potentials of the quasi-reversible couple, respectively.

The bands at ca. 500 and 760 nm are not characteristic of the pyridinyl radicals. With reference to previous spectroscopic work,[6,7b,c,f,l,k,16e] it is suggested that the broad intense band at ca. 760 nm is derived from the intervalence charge-transfer transition of the mixed valence Cu^{I}Cu^{I}Cu^{II} species

$$\mathrm{Cu^ICu^ICu^{II}} + h\nu \rightarrow \mathrm{Cu^ICu^{II}Cu^I}*$$

while the band at ca. 500 nm is likely to be due to a thiolate−copper(II) LMCT transition as similar bands have also been reported in this region for other related systems.[6b−d,16e,18] The transient signal decays via second-order kinetics, in line with the back electron-transfer nature of the reaction. This provides spectroscopic evidence for the electron-transfer quenching mechanism for the bimolecular quenching reactions of the phosphorescent state with pyridinium acceptors.

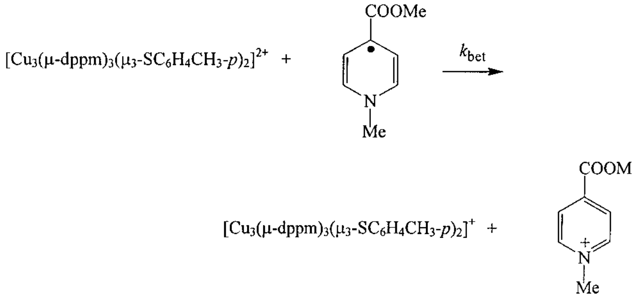

The electrochemistry of complexes **2**−**13** has been studied by cyclic voltammetry, and their electrochemical data are listed in Table 4. All the complexes show a quasi-reversible oxidation couple at +0.54 to +0.74 V vs saturated calomel electrode (SCE). The potential values show trends of **2** > **3** > **4** ≅ **5** ≅ **6** > **7** ≅ **8** and **9** ≅ **10** > **11**, which are in line with the increasing electron-donating ability of the thiolate ligands. In general, the more electron-rich the thiolate ligand is, the less positive the potential of the oxidation couple. The oxidation couples were tentatively assigned as thiolate ligand-centered oxidation in view of the close resemblance of the oxidation potential of **7** and **8** with the same thiolate ligands. Although one could not exclude the possibility of a copper(I)-centered oxidation, which would also give rise to a similar trend, the relative insensitivity of the oxidation potential to the overall charge of the complex and the nature of the monocapped vs bicapped systems as reflected by **7** and **8** would be more in favor of a thiolate ligand-centered oxidation. The oxidation

---

(17) (a) Hermolin, J.; Levin, M.; Kosower, E. M. *J. Am. Chem. Soc.* **1981**, *103*, 4808. (b) Hermolin, J.; Levin, M.; Ikegami, Y.; Sawayanagi, M.; Kosower, E. M. *J. Am. Chem. Soc.* **1981**, *103*, 4795.

(18) (a) Schugar, H. J.; Ou, C.; Potenza, J. A.; Felthouse, T. R.; Haddad, M. S.; Hendrickson, D. N.; Lanlancette, R. A.; Furey, W., Jr. *Inorg. Chem.* **1980**, *19*, 543. (b) Miskowski, V. M.; Thich, J. A.; Solomon, R.; Schugar, H. J. *J. Am. Chem. Soc.* **1976**, *98*, 8344. (c) Ainscough, E. W.; Brodie, A. M.; Husbands, J. M.; Gainsford, G. J.; Gabe, E. J.; Cutis, N. F. *J. Chem. Soc., Dalton Trans.* **1985**, 151.

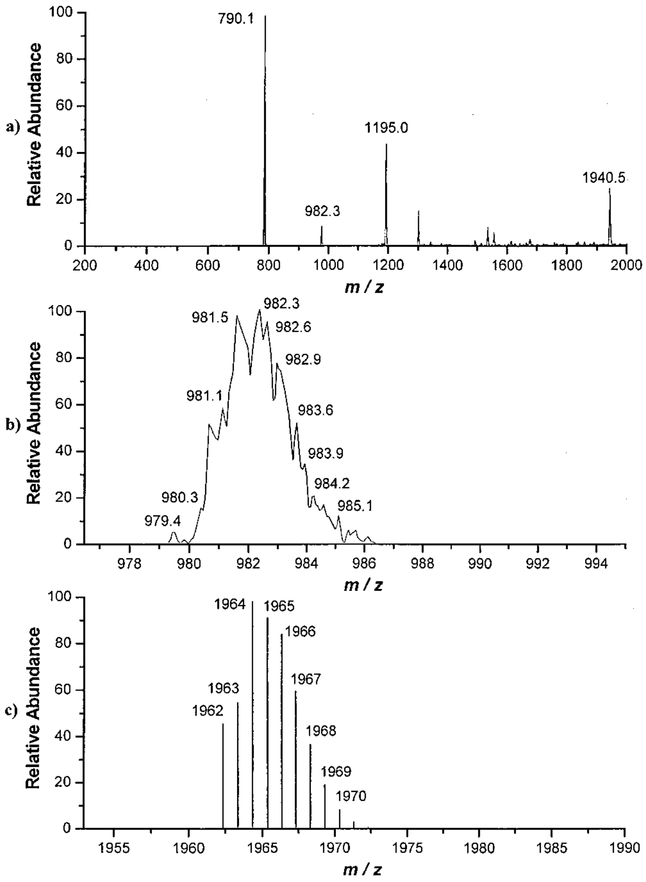

Figure 6. (a) Positive ESI mass spectrum of an acetone solution of **6** and $NaBPh_4$. (b) Ion cluster at *m*/*z* 982, expanded from the positive ESI mass spectrum of an acetone solution of **6** and $NaBPh_4$. (c) Simulated isotope pattern for the adduct $\{[Cu_3(\mu\text{-dppm})_3(\mu_3\text{-S-benzo-15-crown-5})_2]\cdot Na\}^{2+}$.

potentials of the hexanuclear copper(I) selenolate complexes are in the range of +0.70 to +0.74 V vs SCE. No reduction wave was observed even when the potential was scanned to −2.4 V vs SCE. Further oxidation and reduction of the complexes resulted in decomposition, as suggested by the irreversibility of the couples at more anodic and cathodic potentials.

Complex **6** with the mercaptobenzo-15-crown-5 moieties was subject to sodium ion-binding studies. The positive ESI mass spectrum of an acetone solution of **6** and sodium tetraphenylborate is shown in Figure 6a. The ion clusters at *m*/*z* 1941 and 982 correspond to $[Cu_3(\mu\text{-dppm})_3(\mu_3\text{-S-benzo-15-crown-5})_2]^+$ and the sodium ion-bound species $\{[Cu_3(\mu\text{-dppm})_3(\mu_3\text{-S-benzo-15-crown-5})_2]\cdot Na\}^{2+}$, respectively. A simulated isotope pattern and the expanded ion cluster of the sodium ion-bound adduct are shown in Figure 6b,c. No ion clusters corresponding to the 1:2 complexation adduct were observed. The overall 2+ charge of $\{[Cu_3(\mu\text{-dppm})_3(\mu_3\text{-S-benzo-15-crown-5})_2]\cdot Na\}^{2+}$ would not favor further binding of the second sodium ion. Attempts to study the ion-binding properties using UV−Vis spectrochemical methods were unsuccessful because of the limitation of the solvent window of acetone and the solubility of **6** and the sodium salt in organic solvents.

Acknowledgment. V.W.-W.Y. acknowledges financial support from the Research Grants Council and The University of Hong Kong. The receipt of a Croucher Senior Research Fellowship by V.W.-W.Y. from the Croucher Foundation is gratefully acknowledged. C.-H.L. and W.K.-M.F. acknowledge the receipt of a postgraduate studentship, administered by The University of Hong Kong.

Supporting Information Available: X-ray crystallographic files in CIF format for the structure determinations of **12** and **13**. These materials are available free of charge via the Internet at http://pubs.asc.org.

IC0012322